Liquid Crystals
Publication details, including instructions for authors and subscription information:
http://www.informaworld.com/smpp/title~content=t713926090

Microstructure and dynamics of a mesogenic diol

G. Smyth[ab]; S. K. Pollack[ac]; W. J. Macknight[a]; S. L. Hsu[a]
[a] Department of Polymer Science and Engineering, University of Massachusetts, Amherst, Massachusetts, U.S.A. [b] ICI Chemicals and Polymers Ltd., Cheshire, England [c] Department of Materials Science and Engineering and the Polymer Research Center, University of Cincinnati, Cincinnati, Ohio, U.S.A.

To cite this Article Smyth, G. , Pollack, S. K. , Macknight, W. J. and Hsu, S. L.(1990) 'Microstructure and dynamics of a mesogenic diol', Liquid Crystals, 7: 6, 839 — 861
To link to this Article: DOI: 10.1080/02678299008033843
URL: http://dx.doi.org/10.1080/02678299008033843

LIQUID CRYSTALS, 1990, VOL. 7, NO. 6, 839–861

Microstructure and dynamics of a mesogenic diol

by G. SMYTH†, S. K. POLLACK‡, W. J. MACKNIGHT and S. L. HSU
Department of Polymer Science and Engineering, University of Massachusetts, Amherst, Massachusetts 01003, U.S.A.

(*Received 29 June 1989; accepted 9 February 1990*)

A number of techniques have been used to elucidate the structure and dynamics of 4,4′-bis(6-hydroxyhexyloxy)biphenyl (BHHBP) in its various phases. X-ray diffraction studies indicate that the molecules pack in a crystalline phase which melts to produce a highly ordered smectic/disordered crystal mesophase. Based on molecular models and the infrared results, the all trans conformation requires a 45°–55° tilt of the molecules in the smectic layers. Infrared spectroscopic results indicate that a predominantly trans chain conformation and hydrogen bonding of the layered crystal structure persists through the mesophase. Additionally, rotational freedom about the biphenyl linkage appears to occur only in the isotropic phase. NMR data indicate that the alkoxy chain is at or near co-planarity with the respect to the phenyl ring in the crystalline phase, with reorientational motion of the biphenyl group becoming allowed in the mesophase in the form of rapid ($\tau_c \sim 3\,\mu$s at 100°C) small angle liberations and, perhaps, slower ($\tau_c \sim 0{\cdot}5$ ms at 100°C) 180° ring flips. The alkyl chains exhibit a progressive increase in mobility with distance from the biphenyl core and achieve considerable mobility at the hydroxy end of the chain despite the fact that hydrogen bonding still occurs in the mesophase.

1. Introduction

The classification, structure and phase behaviour of liquid crystal and disordered crystal mesophases has been an active and growing area of research interest over many years [1–8]. Although major interest still focuses on the structure of these mesophases the investigation of the re-orientational dynamics of molecules in these phases has also attracted attention [7–11].

As part of an ongoing study of thermotropic mesomorphic polymers [12], we have become interested in the way in which the structure and dynamics of mesomorphic polymers relate to their small molecule analogues. In this regard we report upon the results of investigations into the structure and dynamic behavior of a monomeric mesogen 4,4′-bis(6-hydroxyhexyloxy)-biphenyl (BHHBP):

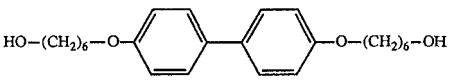

which has been used as the mesogenic unit in the synthesis of polyurethanes [13–15], polyesters [16, 17], and polycarbonates [18] which in all cases have been observed to exhibit smectic-like phases.

† Permanent address: ICI Chemicals and Polymers Ltd., P.O. Box 8, The Heath, Runcorn, Cheshire WA7 4QD, England.

‡Permanent address: Department of Materials Science and Engineering and the Polymer Research Center, University of Cincinnati, 498 Rhodes Hall, Cincinnati, Ohio 45221-0012, U.S.A.

0267-8292/90 $3.00

In the present study differential scanning calorimetry, optical microscopy, X-ray diffraction, infrared and ^{13}C NMR spectroscopy are applied to the investigation of the BHHBP. Although a complete three dimensional structure is not available for this molecule, considerable insight into the structure can still be obtained from the combination of different experimental techniques. Infrared and NMR spectroscopy are additionally useful in the investigation of dynamic aspects of BHHBPs behaviour in the mesophase.

2. Experimental

The synthesis of the BHHBP has been described in detail elsewhere [13, 16]. Briefly, 4,4′-dihydroxy-1,1′-biphenol was suspended in an excess of ethanolic NaOH and 6-chloro-1-hexanol was added with stirring. The reaction was refluxed overnight, and the products purified by recrystallization from *n*-butanol or *n*-butanol/dioxane mixtures.

Differential scanning calorimetry was performed on a Perkin–Elmer DSC-7 employing a 20 ml/min flow of dry nitrogen gas to purge the sample and reference cells, and an ice–water bath as coolant. The temperature and power ordinates of the instrument were calibrated using the melting point and heat of fusion of a high purity indium sample as a reference. Sample weights were typically in the range of 7–10 mg.

Optical microscopy was performed on an Olympus polarizing microscope with Koffler hot stage and Omega temperature controller.

X-ray diffraction data were obtained using Ni filtered Cu Kα radiation and a Statton type flat film camera. Exposure times were on the order of 2·5 hours.

Infrared spectroscopy was performed using a Bruker IFS 113v Fourier transform spectrometer. Samples were measured in transmission as KBr pellets (1 per cent w/w). Experiments at elevated temperatures were performed using a temperature controlled heating cell.

Nuclear magnetic resonance (NMR) measurements were performed on a Bruker AF200 spectrometer equipped with high power IBM Instruments solids accessories and a Doty Scientific ^{13}C selective magic angle sample spinning probe for solid state spectroscopy. The spectrometer was operated at a carbon frequency of 50·323 MHz with Hartman–Hahn matched decoupler and transmitter rf-field strengths of 55·56 kHz. For NMR, samples in the form of fine powder were packed into sapphire rotors which were fitted with Kel-F® or ceramic end caps. Sample spinning was by means of a compressed air supply which allowed spinning rates of up to 4·5 kHz to be achieved. For variable temperature work a Bruker BST-700 temperature controller was used to heat the spinner gas and control the sample temperature to $\pm 2°C$ at temperatures from 20°C to 120°C—the upper temperature limit for the probe used in this study.

The standard cross-polarization/dipolar–decoupling/magic angle sample spinning (CP/DD/MASS) pulse sequence [19] which in the present instance employed with a 2 ms cross-polarization time and 3 s recycle delay was supplemented by using short contact time [20] (SC) and dipolar dephasing [21] (DD) pulse sequences to discriminate among various carbon types on the basis of their ^{13}C–^{1}H dipolar couplings. The SC sequence differed from the CP sequence only in the use of a much shorter cross-polarization time of 20 μs, while the DD sequence differed only by the insertion of a short (50 μs) delay between the end of the CP sequence and the onset of high power proton decoupling and data acquisition.

Molecular geometries and minimum energy dimer structures were calculated using the Biograf™ (Molecular Design, Inc., Pasadena, California) with the Dreiding force field [22] operating on a Silicon Graphics Incorporated Personal Iris.

3. Results and discussion

For bulk BHHBP the changes that occur in the packing of molecules as a function of temperature reflect a change in the balance between the strength of interactions between molecules and the amount of motion or disorder imparted to different moieties within the molecule. In addition to the dispersive interactions between the aromatic cores which stabilize the lateral ordering between molecules, there are specific interactions in the form of hydrogen bonds between the terminal hydroxyl groups with other hydroxyl groups or with the phenyl ether linkage. Changes in packing are most easily observed in changes in X-ray diffraction patterns. The changes in the conformations of the individual structural units of the molecule which occur in going from one phase to the other and help to dictate the packing scheme are better observed by spectroscopic techniques, such as vibrational and NMR spectroscopy. The motion of the various functionalities within the molecule in the various phases can be readily monitored by NMR techniques. All these are applied in this study in trying to understand the properties of BHHBP as a function of temperature and physical state.

Before describing the structural characteristics of this compound, an understanding of the phase behaviour of BHHBP is necessary. The thermal behaviour of BHHBP was characterized by DSC. Heating and cooling traces recorded at 10°C/min are shown in figure 1, and the transition parameters associated with these traces are summarized in table 1. Two first order transitions are apparent on the heating trace. The higher temperature endotherm at 179°C is unambiguously associated with the transition to the isotropic melt. The lower temperature endotherm at 98°C must therefore be associated with a transition to a state of order which is intermediate between that of the room temperature crystal phase and the isotropic melt. The fact that the higher temperature transition has larger transition entropy than its lower temperature counterpart indicates that, although some disordering occurs at the lower temperature transition, major disordering is postponed until the isotropization temperature. In fact, when account is taken of the various contributions [2, 23] from positional disordering, $\Delta S_{pos} \approx 7$–$14\,J\,mole^{-1}\,K^{-1}$, orientational disordering, $\Delta S_{orient} \approx 20$–$50\,J\,mole^{-1}\,K^{-1}$, and form configurational disordering, $\Delta S_{conf} \approx 105$–$180\,J\,mole^{-1}\,K^{-1}$ (based on 15 flexible bonds), it is clear that there must be a significant contribution to the isotropization transition from configurational disordering. Conversely, there must be little configurational disordering in going from the crystal

Table 1. BHHBP thermal transition data†.

	Temperature		ΔH		ΔS	
Cycle	°C	K	$J\,g^{-1}$	$kJ\,mole^{-1}$	$J\,g^{-1}\,K^{-1}$	$J\,mole^{-1}\,K^{-1}$
(*a*) Heat	97·9	371·1	55·8	21·6	0·150	58·1
	178·8	452·0	114·7	44·3	0·253	98·1
(*b*) Cool	85·3	358·5	−48·2	−18·6	–	–
	168·7	441·9	−112·1	−43·3	–	–

† Obtained by DSC at 20°/min scanning rate.

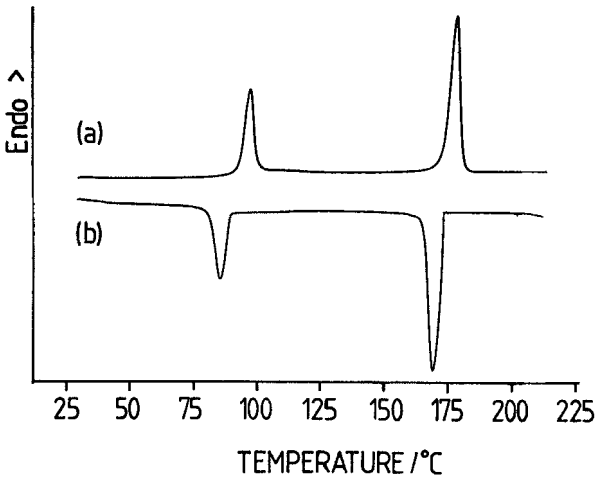

Figure 1. DSC heating (*a*) and cooling (*b*) traces for BHHBP recorded at 20°C/min.

phase to the mesophase, based on the observed values of the entropy for this transition (table 1). It is noted that the exotherms which appear in the cooling cycle exhibit only a small degree of supercooling by comparison with their corresponding endotherms on the heating cycle.

The nature of the BHHBP phase between 98°C and 179°C is further illuminated by optical microscopy. Upon cooling from the isotropic melt the distinctive mosaic texture shown in figure 2 (*a*) develops at *c.* 180°C. The material is mobile but highly viscous in this state. At the early stages of growth from the isotropic melt, these mosaic domains exhibit a coarse dendritic growth pattern. As the temperature is further reduced the material between the glass slides begins to fracture at *c.* 40°C below the isotropic to mesophase transition due to stresses induced by the differential contraction of the glass substrate and the sample. This produces a pattern of crazes which intersect at regular angles as is shown in figure 2 (*b*). The crystalline phase, observed at 23°C has the same overall appearance as the mesophase but there are fine striations observed in the individual domains. Upon heating this sample, the fine striations disappear at the crystal to mesophase transition and at the upper end of the temperature interval between the two transitions, the crazes which formed during the cooling cycle were observed to 'heal'.

The observation of low undercooling, mosaic texture, and plastic behaviour coupled with the relatively small entropy of the 98°C transition suggest that between 98°C and 179°C BHHBP exhibits a stable highly ordered mesophase. Here the term 'highly ordered mesophase' is used to denote the highly ordered smectic and disordered crystal phases [2, 4] which exhibit many of the properties outlined above.

The X-ray scattering pattern can now be examined in the light of the observed transition temperatures and the microscopic texture analysis. Powder X-ray diffraction patterns taken in the crystal phase and the mesophase are shown in figure 3. Both exhibit a number of strong relatively sharp reflections. In the molten state, at 180°C, only a weak amorphous halo is observed. While a magnetically oriented mesophase would aid in interpretation of the X-ray scattering, no attempts to produce oriented samples were made, as magnetic fields of appropriate strength (> 1 Tesla) to achieve orientation of the mesophase were not available for this study. Still, much

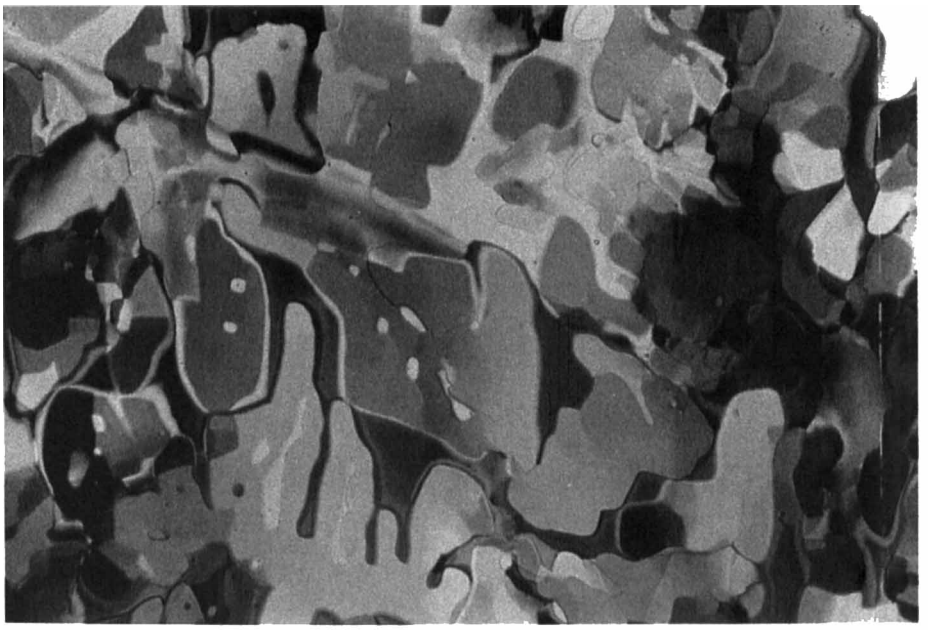

(*a*)

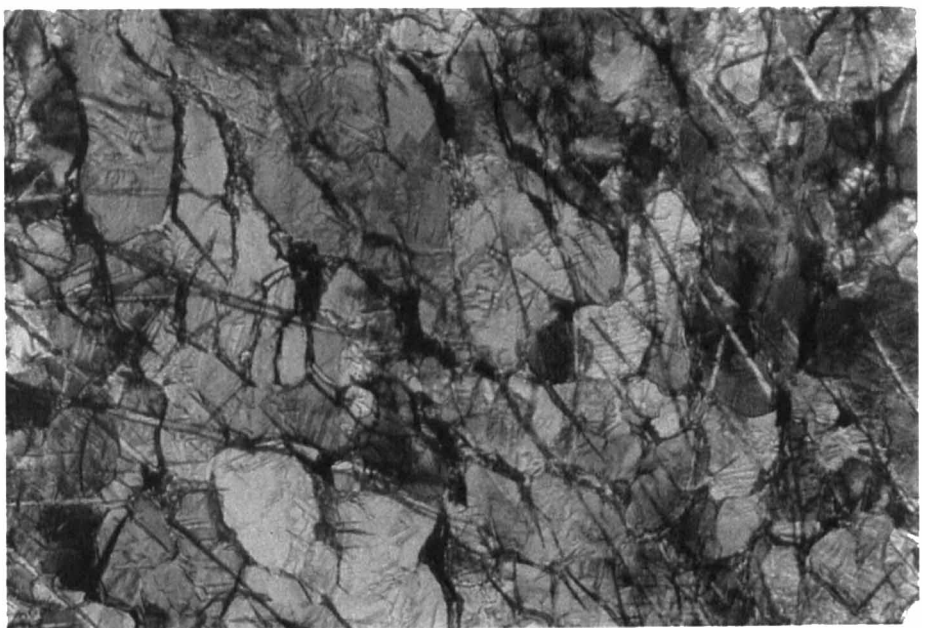

(*b*)

Figure 2. (*a*) mosaic texture of **BHHBP** obtained on cooling from the isotropic melt to *c.* 180°C. (*b*) Fracture pattern observed at 23°C after cooling sample with texture shown in (*a*) to room temperature.

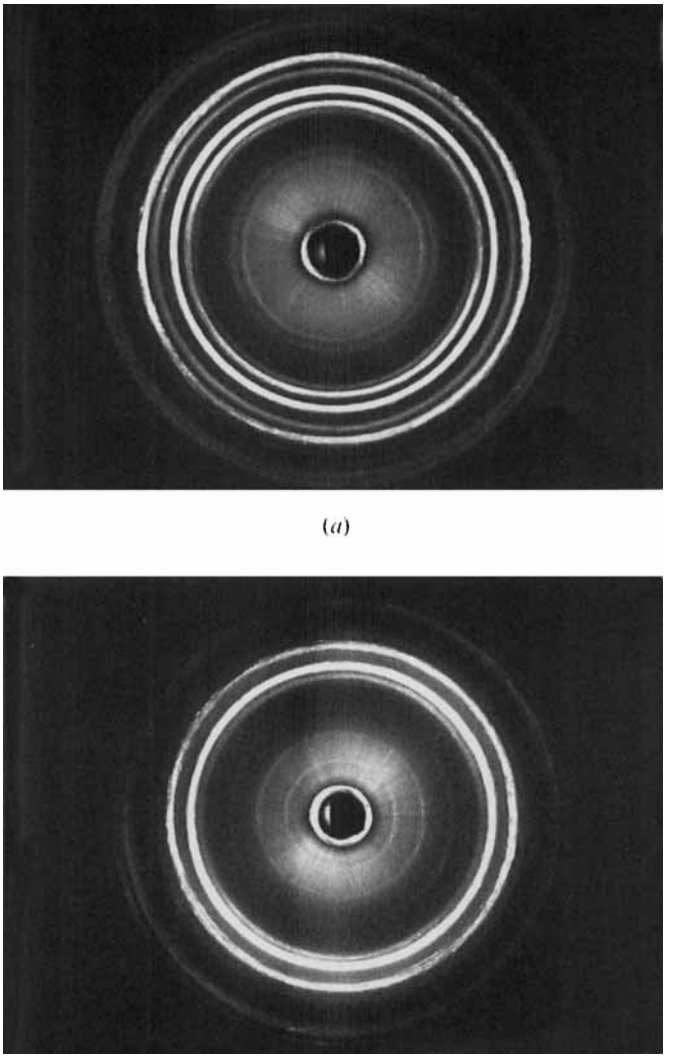

(*a*)

(*b*)

Figure 3. X-ray powder diffraction patterns of BHHBP sample at (*a*) 23°C and (*b*) after heating to 130°C. Exposure times were roughly 1·5 hours.

information can be obtained from the powder patterns. Table 2 lists the spacings for the reflections observed in the two phases. In both phases, there is an inner reflection corresponding to a *d* spacing of 22–23 Å. This reflection is assigned to the layer spacing in a smectic mesophase. It is interesting to note that there is little change of this distance in going from the crystal to the mesophase. Based on molecular modelling using standard bond lengths [22] and assuming an all trans configuration for the hexamethylene chains, the oxygen–oxygen distance of BHHBP is calculated to be 26 Å. The terminal hydrogen–hydrogen distance is calculated to be 28 Å. The addition of hydrogen bonds observed in the infrared spectra (see below) would further serve to increase the spacing between adjacent molecules along the long axis of the molecule, assuming that the hydrogen bonds occur between the molecular layers and not within

Table 2. Major reflections (Å) for powder patterns of BHHBP in crystal and mesophase. Relative intensity in parenthesis.

Temperature	
23°C	150°C
2·9 (weak)	–
3·0 (med)	–
3·1 (med)	–
–	3·3 (weak)
3·6 (strong)	3·6 (weak)
3·8 (strong)	3·8 (strong)
4·2 (med)	–
–	4·4 (strong)
4·6 (strong)	4·6 (weak)
4·8 (strong)	–
6·5 (weak)	–
7·3 (faint)	–
22·1 (med)	23·0 (med)

the layers. Given these distances and the observed 22–23 Å spacing in the X-ray, both the crystal phase and the mesophase must encorporate a considerable tilt of 45°–55° to accommodate the fully extended molecule (figure 4). Any chain compression, caused by gauche sequences in the alkyl chains would allow for a decreased tilt. As will be shown from the infrared studies (below), the chain is a mostly trans conformation both in the crystal and the mesophase suggesting a tilted smectic phase.

There are, of course, two hydrogen bonding acceptor sites available on each chain, the hydroxyl and the phenyl ether oxygens. The consequences of the two types of hydrogen bond geometries lead to significantly different three dimensional structure for the packing of molecules. If the hydrogen bonds are between the terminal hydroxyl hydrogen and the hydroxyl oxygen of the next molecule, a layered structure would develop, with the tilt of the molecular axis relative to the layer normal mentioned above accounting for the difference between the length of the molecule and

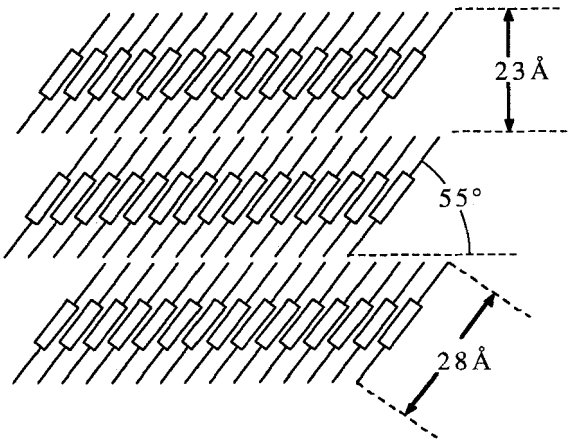

Figure 4. Schematic of layered packing arrangement of BHHBP assuming fully extended alkyl chain.

Table 3. Band asignments for BHHBP infrared spectrum as a function of temperature.

Frequency/cm^{-1}			
23°C	95°C	165°C	Assignment†
3380	3400	3523	O–H · · · H stretch
–	–	3601	O–H stretch
3068	3067	3061	Ring C–H stretch
3041	3039	3035	Ring C–H stretch
2959	–	–	Fermi resonance
2940	2937	2938	$\nu_{as}(CH_2)$
2929	–	–	Fermi resonance
2915	–	–	
2874, 2864	2860	2863	$\nu_s(CH_2)$
1607	1605	1605	Ring C=C stretch
–	1582	1581	Ring C=C stretch, perpendicular biphenyl conformer
1568	1567	1565	Ring C=C stretch
1500	1500	1497	Ring C=C stretch
1480	–	–	δCH_2
1475	1475	–	δ_{CH_2}, B_{3u} biphenyl
–	1470	1470	Ring mode
1464	–	–	δ_{CH_2} (crystal)
1454	1454	–	δ_{CH_2}
1440	–	–	δ_{CH_2} (gg)
–	1431	1433	
1421	–	–	O–H ipb
1403	1404 (sh)	–	
1395	1394	1389	
1379	–	–	ω_3
1355	–	–	
1328	1326	–	O–H ipb, δ_{CH_2}
–	–	1311	O–H ipb
1300	–	–	
–	–	1283	CH_2–O–H asymmetric stretch
1273	1273	–	CH_2–O–H · · · O asymmetric stretch
–	–	1267	
1249	1246	1238	Ph–O–CH_2 symmetric stretch
1212	–	–	
1208	–	–	
1179	1178	1172	Ring C–H ipb
1172	–	–	ω (cryst)
1139	1136	–	C–C stretch
1122	1120	–	
1105	–	–	
1078	1074 (sh)	–	Ph–O–CH_2 symmetric stretch
1065	1056	1056 (sh)	R_2
1042	–	–	
1035	1034	1035	R_3
1026	–	–	$\gamma_r(CH_2)$
1004	1008	1011	Phenyl-phenyl stretch
995	995	997	
986	987 (sh)	997	
952	952 (wk)	–	
938	933	934	P
917	917 (wk)	–	

Table 3 (*continued*).

Frequency cm^{-1}			
23°C	95°C	165°C	Assignment†
870	871 (wk)	–	
829, 823	823	821	Ring C–H oop bend
806	807	806 (sh)	P
761	760 (wk)	–	P
736, 727	–	–	P (crystal) (progression)
–	731	732	P GT_mG ($m > 2$)
712	710	713 (sh)	
675 (br)	–	–	COH · · · O oop bend
646	646	642, 632	Ring B_{2u}
594	593	594	Ring skeleton oop
526	–	–	Ring B_{2g}
516	516	523	Ring B_{2g}
508	510 (sh)	–	Ring B_{2g}

† Symbols: ν, CH stretch; δ, CH_2 bend, ω, CCC bend, γ, CCH bend, R, CC stretch, P, CH_2 rocking mode progression band.

the thickness of the layers. For structures of the type:

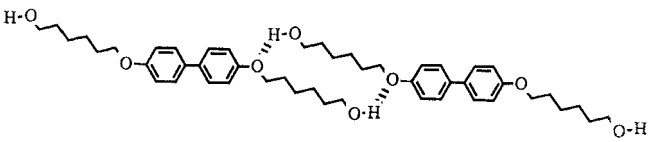

the distance from one biphenyl group to the next would also be on the order of 21–22 Å, not requiring a tilt. However, using simple molecular mechanics [22] which includes potential terms for the hydrogen bonding interaction, it was found that for this type of packing, steric repulsion between the alkyl chains dominates, giving a hydrogen–oxygen distance for the hydrogen bond of 4·75 Å, far too long to be considered a real hydrogen bond. Given this observation, a structure with hydrogen bonds between terminal hydroxyl groups, leading to a layered structure is the most probable.

There is a reduction in the number of reflections near 20° (d spacing of roughly 3·6–4·8 Å) in going from the crystalline phase to the mesophase. If a simple smectic phase (S_A or S_C) were present, the X-ray scattering would exhibit only a diffuse ring at 20°, corresponding to the liquid-like packing of the molecules within the layers. The fact that there remains a number of sharp reflections in the mesophase suggests lateral ordering within the smectic layers. A number of tilted smectic phases have higher of order within the smectic layers [5]. Attempts to fit the observed reflections to an orthorombic array proved unsuccessful, precluding an assignment of a S_E phase. Thus, we tentatively assign the observed phase as either a S_G or S_H.

While X-ray diffraction gives a picture of the long range order and arrangement of the individual molecules, it does not readily give a measure of the order and mobility of the various moieties within the molecules. A number of studies of low molar mass liquid-crystalline molecules have utilized infrared spectroscopy to characterize the changes that occur both in the conformations of the alkyl chains as well as the mobility of the mesogens and alkyl chains in the different phases these molecules exhibit [24–27]. Figure 5 gives the infrared spectrum of BHHBP at a number of

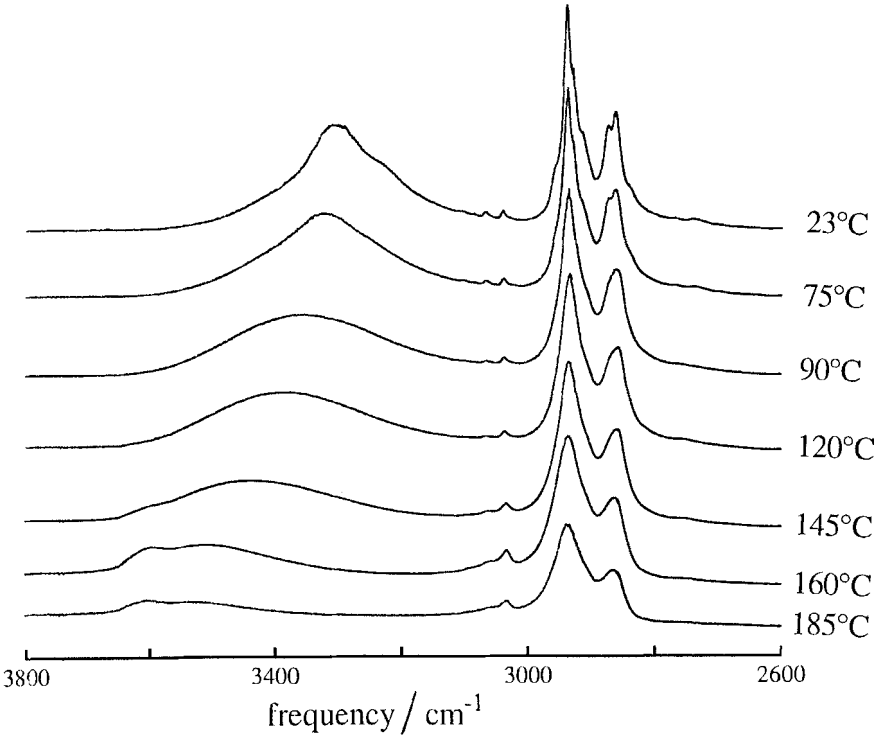

(*a*)

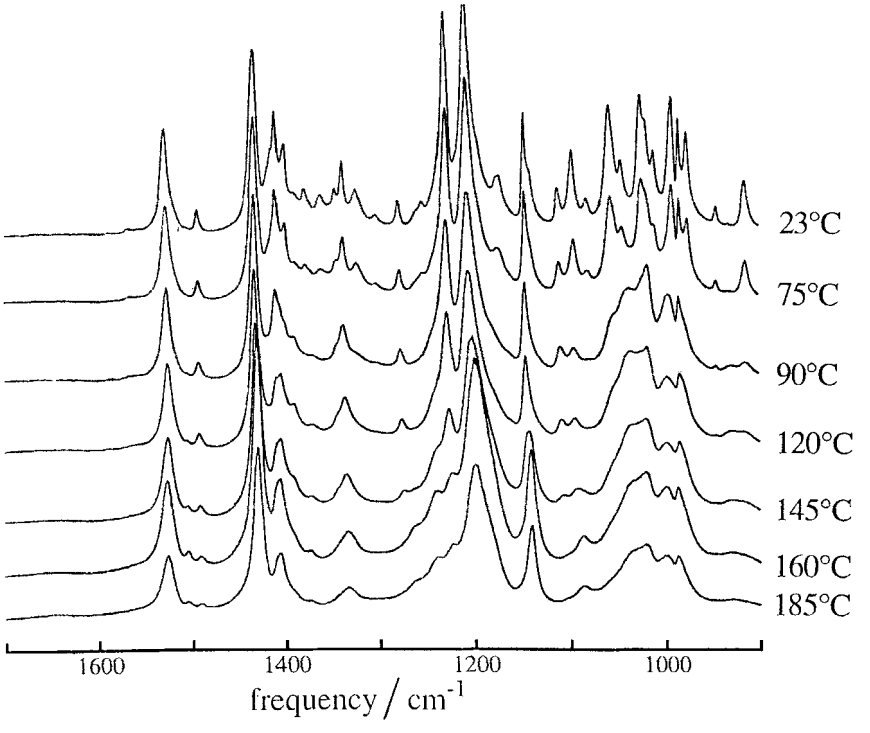

(*b*)

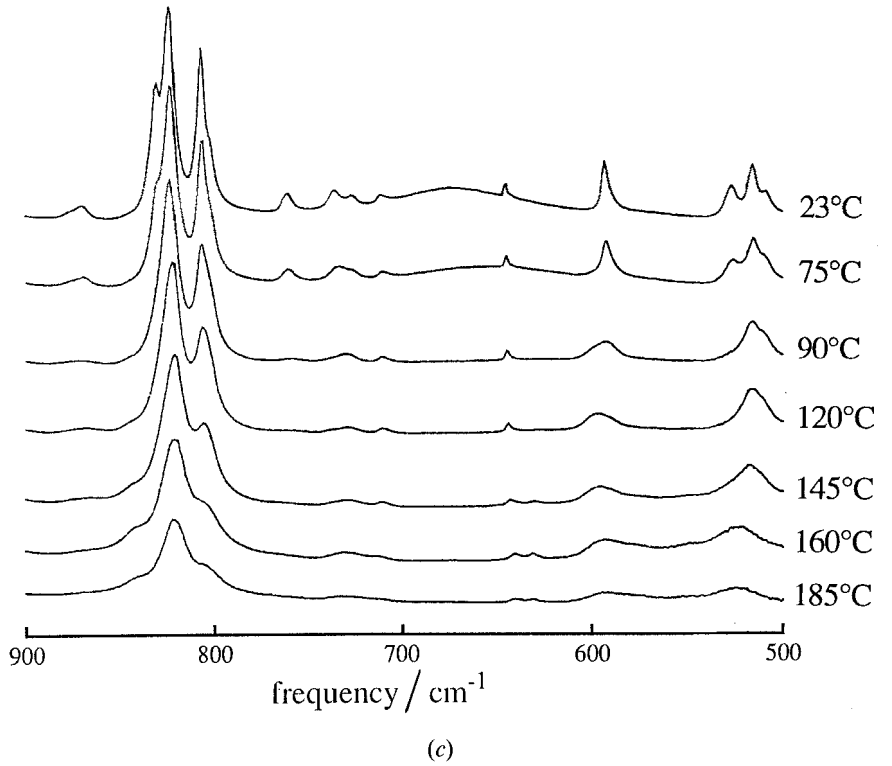

(c)

Figure 5. Infrared spectra of BHHBP at indicated temperatures.

temperatures within all three of its phases. Table 3 contains the frequencies and assignments of many of the bands in these spectra [28–30, 32]. As anticipated for hydrogen bonded systems, the OH stretch is a broad band centred at 3380 cm^{-1} in the crystalline phase. As the temperature increases, the band broadens further and its intensity decreases due to the change in the distribution of hydrogen bonded geometries [29]. At 145°C the first evidence of a non-bonded OH stretching vibration occurs, with a new peak developing at 3601 cm^{-1}. Examination of other hydrogen bonding related bands also show the persistance of hydrogen bonding through the mesophase. For example, the C–O–H asymmetric stretch, located at 1273 cm^{-1} broadens in the mesophase, and all but disappears as the sample becomes isotropic.

There is a broad band (FWHM of 75 cm^{-1}) which is observed in simple alcohols at 675 cm^{-1}. It is assigned to the hydrogen bonded OH out of plane bend [30], and in BHHBP loses all intensity upon entering the mesophase. There is also an indication of a shift to lower frequency with increasing temperature, again indicating a re-distribution of population to geometries with weaker interactions. This band reappearns upon cooling through the mesophase–crystal transition.

Examination of the vibrations associated with the aliphatic side chains should allow for the probing of the onset of motion and disorder in this part of the molecule as a function of temperature. In a number of studies [24, 25], there has been noted significant disordering prior to the optically and thermally observed transitions. At 23°C, there is a significant coupling of the C–H stretching with the lower frequency bending and rocking modes through Fermi resonance [27]. At 75°C, 23° below the transition temperature, a decrease in the intensity of the Fermi resonance bands is observed in the region from 2800–3000 cm^{-1}. Also observed is a decrease in the

intensity of a number of CH_2 bending (1468 cm^{-1} in C_4H_{10}) [28] and rocking progression bands (P_1 at 733 cm^{-1} and P_3 at 942 cm^{-1} in C_4H_{10}) [28] associated with the crystal phase. Many of these bands may be associated with crystal field splitting, but given the lack of a crystal structure, a detailed analysis is not possible.

Galbiati and Zerbi have noted that as the dodecylcyano biphenyl [24] and dodecyloxycyano biphenyl [25] systems undergo phase transitions from the crystal phase to the smectic phase, defect bands in the wagging region due to the development of gauche rotomers. We have attempted to use Zerbi's technique of temperature difference spectra to look for the presence of gauche related bands developing upon entering the mesophase. However, equivalent bands are not observed for the crystal–mesophase transition in BHHBP. This may be due to the relatively short methylene sequences (C_4, discounting the terminal oxymethylenes) in BHHBP relative to those in the dodecyloxy- and dodecylcyano biphenyl. These workers also observe a reduction in the Fermi resonance bands in going from the crystal to the smectic phase, consistent with the behaviour of BHHBP. The rocking mode decreases only slightly in intensity (807 cm^{-1}) upon going from the crystal to the mesophase. The band loses most of its intensity as the material goes into the isotropic phase. The loss of peak height and broadening upon entering the isotropic phase is most likely due to an increase in the population of conformers with different rocking mode frequencies. Based on these observations, it is proposed that the aliphatic chains are in a predominantly trans configuration in the crystalline phase and develop slight disorder in the mesophase, enough to remove any crystal field splitting. It is not until the isotropic phase is reached that the chains completely disorder. This is completely consistent with the X-ray observations. These data indicate that the length of the chain does not change significantly in going from the crystal phase to the mesophase, based on the small changes observed in the *d* spacing for the long reflection (from 22 Å to 23 Å).

The behaviour of the mesogenic biphenyl unit is also of interest. The biphenyl ring has three potential degrees of mobility: that due to torsions about either of the two alkoxy linkages and the potential of torsions of the biphenyl ring–ring linkage. There are splittings of the ring C–H out-of-plane bending modes in the crystal phase as well as of the ring skeletal out-of-plane modes which are eliminated upon going from the crystal to the mesophase (829–821 cm^{-1} and 550–500 cm^{-1} respectively). A similar change is observed in the aromatic combination bands observed at 1850–1750 cm^{-1} (figure 6).

In addition to the disappearance of bands as the material goes from the mesophase to the isotropic phase, two bands which are in the region for ring related vibrations develop. Above 120°C, a weak band in the aromatic C–C stretching region at 1582 cm^{-1} increases in intensity. Also observed is a band in the ring deformation region at 632 cm^{-1}. It is tempting to assign these bands to ring modes for non-planar conformations of the two rings. These conformations are at another potential energy minimum for biphenyl [31–33], in addition to the nearly co-planar conformation normally exhibited in the crystal phase. Schmid and Brosa [33 (a)] have determined a correlation between the twist angle between the aromatic rings of biphenyl and the intensity of the Raman active ν_{16a} and ν_{16b} ring vibrational modes of the phenyl rings. Unfortunately, our attempts to obtain useful Raman scattering data from our samples proved unsuccessful, due to a highly fluorescent background.

In summary, the infrared results tend to indicate that upon entering the mesophase, the molecule develops some positional disorder, but the side chains remain in a predominantly trans conformation. The fact that this sort of behaviour is not

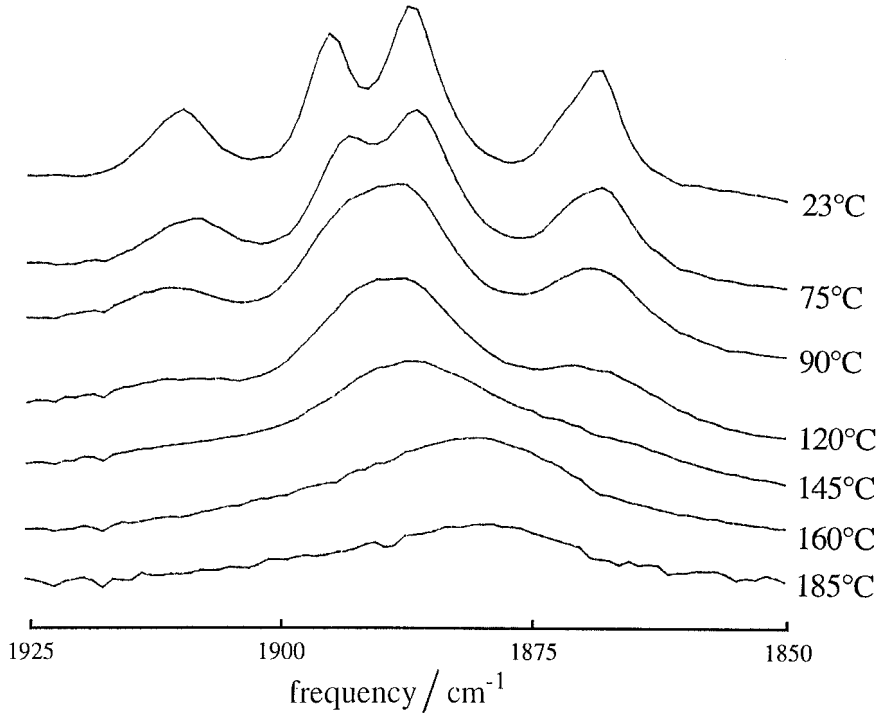

Figure 6. Infrared spectra of aromatic overtone region at indicated temperatures.

observed in the cyanobiphenyl systems mentioned earlier [24 25] is most likely due to the strong interaction of the terminal hydroxyl functions acting to stabilize the terminal end of the chain, while the interaction of the mesogens anchor the other end of the chain. In the case of the cyanobiphenyl systems, there is no specific interaction available to stabilize the terminal end of the chain, making the disordering process more facile.

Solid state ^{13}C NMR spectroscopy was performed with a view toward obtaining information pertaining to the structure and dynamics of BHHBP in the crystal and mesophase states. In order to aid in the assignments of the solid state ^{13}C NMR spectra a preliminary analysis of a solution spectrum was performed. Line positions and assignment for the solution spectrum are summarized in table 4. The carbon resonances are relatively easy to assign as the line positions are consistent with the predictions of simple linear additivity relations for phenyl and linear alkyl substituents [35] (see table 4). In the case of the aliphatic carbons the assignments for 1-hexanol and 4-hexyloxyaniline were used as references [36]. It must be noted however that owing to the small (0·2 ppm) difference between the lines assigned to carbons 3 and 4 the order of assignment for this particular carbon pair cannot be made unambiguously.

Turning now to the CP/DD/MASS studies of bulk BHHBP the solid state spectrum recorded at room temperature is shown in figure 7 with corresponding line assignments given in table 4. The line assignments in this case are made by analogy with the solution spectrum and are consistent with the results of short contact time and dipolar dephasing experiments which identify the various protonated and non-protonated carbon species. It may be noted that the spinning sidebands from the

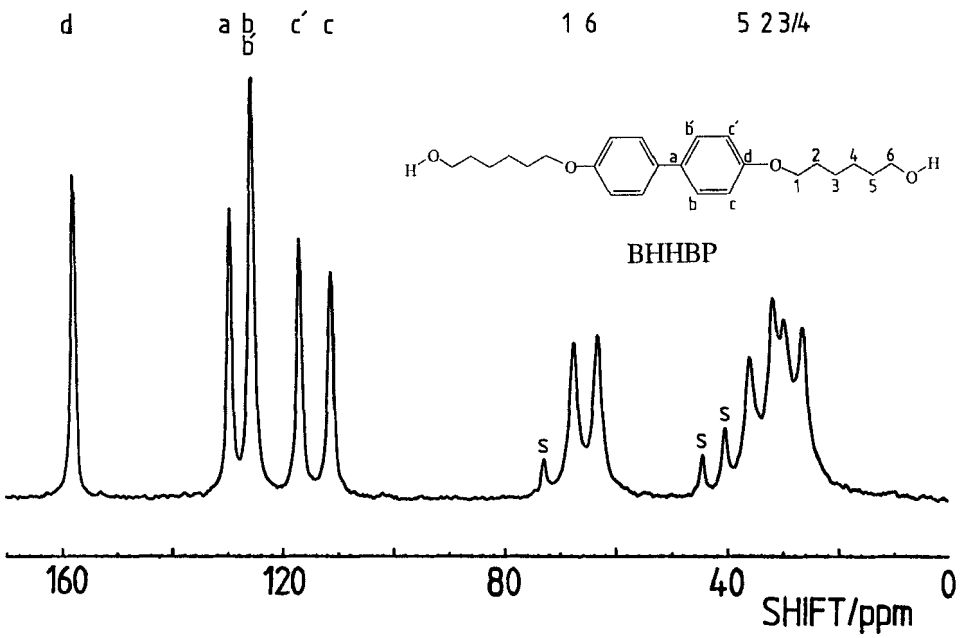

Figure 7. CP/DD/MASS ^{13}C NMR spectrum of BHHBP at 20°C. Peaks denoted s are due solely to spinning sidebands.

aromatic carbons do not affect the aliphatic carbon line positions. This was verified both by varying the sample spinning rate and by employing a direct polarization sequence which, owing to the very long aromatic carbon T_1s, results in a spectrum completely free of the aromatic carbon lines and their associated spinning side bands.

Comparison of the solid state spectrum with the solution spectrum (table 4) reveals, however, that despite the general consistency between these two spectra there are also a number of significant differences. There is a general tendency for the aromatic carbon lines to resonate at slightly higher fields in the solid state compared to solution. This increased shielding is most probably due to steric effects arising from the close packing of molecules in the solid state and perhaps also to a tendency for stacked phenyl rings to shield each other. More striking is the splitting of the aromatic

Table 4. BHHBP ^{13}C chemical shift assignment.

Assignment	Predicted ppm (solution)	Solution ppm 20°C	Solid ppm 20°C	Mesophase ppm 100°C
d	158·9	157·7	157·3	157·5
a	133·7	132·2	129·0	129·2
b/*b'*	128·4	127·1	124·9	125·5
c/*c'*	114·6	114·8	110·1/116·3	114·1
1	69·6	67·4	67·1	67·7
6	62·6	60·6	62·7	62·6
5	32·6	32·4	35·2	33·2
2	29·4	28·7	30·8	30·8
3(4)	25·7	25·4	25·7	27·1
4(3)	25·5	25·2	28·9	27·1

carbon resonances due to carbons *c* and *c'* which are ortho to the oxygen bond of the biphenyl. The inequivalence of these two carbons is due to a locking of the alkoxy carbon 1 in or close to the plane of the adjacent phenyl ring. By way of contrast the resonances for this carbon pair appears at a central position in solution since rapid re-orientation about the oxygen phenyl bond makes the ortho carbons equivalent from an NMR perspective. Similar splitting of aromatic ring carbons due to the locked configuration of substituents has been reported by Lippmaa *et al.* [37], and by Maricq and Waugh [38] for solid dimethoxy benzene, and by Uryu and co-workers [39–41] in a variety of thermotropic polyesters and model compounds.

In the aliphatic region of the spectrum it is observed that, with the exception of the lines at 67·1 ppm and 25·1 ppm, all of the other lines exhibit significant downfield shifts compared to their positions in solution. Leaving aside for the moment consideration of the 25·7 ppm solid state line, the de-shielding of the other aliphatic carbons is consistent with the all trans configuration of the aliphatic spacer which was deduced from the infrared study. Gauche conformations in an aliphatic chain generally produce a shielding effect—the so called γ-gauche effect [42, 43]—which shifts the resonance of carbons which have a γ-carbon in a gauche conformation upfield by *c.* 5–6·5 ppm compared to the trans configuration. In solution rapid gauche–trans fluctuations occur and the aliphatic line positions are weighted according to the relative populations of gauche and trans species and thus generally occur 2–3 ppm upfield compared to the trans conformation. The comparatively small difference between the solution and solid state shifts for carbon 1 can be accounted for in terms of the shielding conformation which this carbon experiences in the solid owing to its locked conformation with respect to the biphenyl ring [40].

Returning now to consideration of the solid state line at 25·7 ppm it is first noted that the assignments for this line and the line at 28·9 ppm are tentative since the corresponding solution lines are separated by only 0·2 ppm. Here it is noted that irrespective of the assignment of the 25·7 ppm line to carbon 3 or 4, the lack of a significant downfield shift compared to the corresponding solution line is not consistent with the overall trend of the other aliphatic carbons. One possibility to account for this would be to postulate a rotation of the 6 carbon about the 5–6 bond to bring the hydroxy group out of the plane of the alkyl chain toward a gauche type conformation leading to a γ-shielding effect between the hydroxyl group and carbon 4. A similar interaction between carbon 3 and its nearest oxygen atom could also be invoked of course. In any event, resolution of the anomalous shift of the 25·7 ppm line in the solid state msut rely on more detailed structural information than is presently available.

Variable temperature ^{13}C NMR spectra were acquired using standard cross polarization (CP), short contact time (SC), and dipolar dephasing (DD) pulse sequences in order to discriminate among the various carbon species on the basis of their ^{13}C–^{1}H dipolar couplings. The half times required for the various carbon species to polarize were also determined at 20°C and 100°C using a variable contact time CP sequence since these data are complementary to the SC sequence and also contain information about the carbon–proton dipolar couplings [44, 45]. It was anticipated that information concerning the relative mobility of the subunits of BHHBP could be obtained in this manner since the strength of the ^{13}C–^{1}H dipolar interaction is sensitive to molecular motion. Earlier studies by Lauprêtre *et al.* [47, 48] have demonstrated the utility of cross-polarization time ($t_{1/2}$) measurements for studying molecular motion in solid polymers. It has, moreover, long been recognized that certain protonated

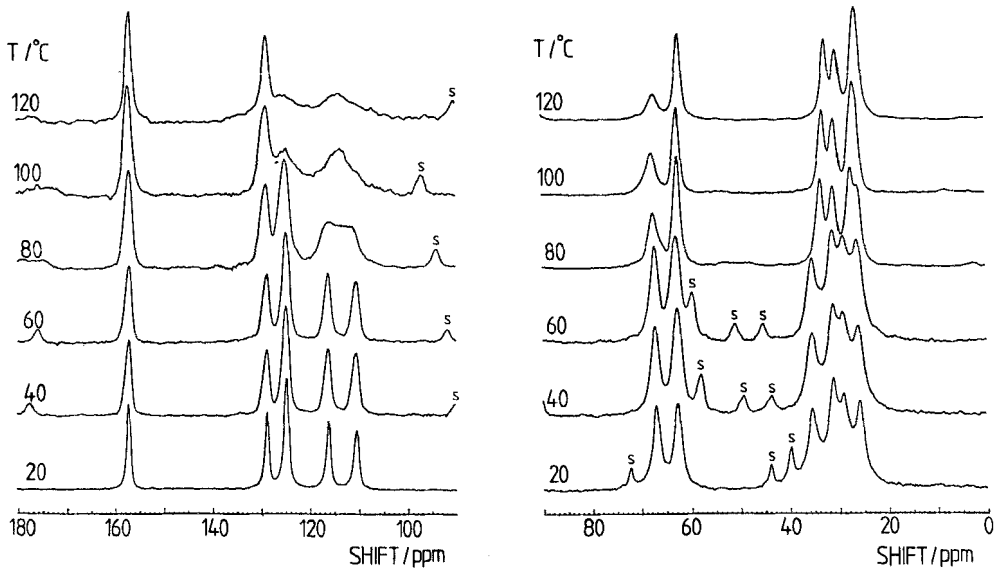

Figure 8. Variable temperature CP ^{13}C spectra for BHHBP. The peaks denoted s are due solely to spinning sidebands.

carbon species preferentially survive the DD sequence owing to reduction of their ^{13}C–^{1}H interaction strength by rapid re-orientational motions [20, 21].

The strength of the ^{13}C–^{1}H interaction is characterized by the truncated Van Vleck second moment of the interaction [46, 49], M_2^{CH}, which can be readily calculated in the rigid lattice if the C–H bond lengths and the distribution of bond angles relative to the applied magnetic field are known. Reductions in the strength of the ^{13}C–^{1}H interaction owing to molecular motion are reflected in the reduction of the second moment, M_2^{CH}, which can be calculated explicitly for various molecular reorientational motions [45, 46, 48].

Spectra obtained from the various pulse sequences outlined above are presented in Figures 8–10. Chemical shift versus temperature data gleaned from these spectra are presented in figure 11. For the sake of comparison with the solution and solid state spectra, table 4 also includes carbon shifts determined in the mesophase at 100°C. Cross polarization time data for the various carbons determined at 20°C and 100°C are presented in table 5.

Table 5. Cross polarization times ($t_{1/2}$) for BHHBP carbons.

	Cross polarization times/μs						
Temperature/°C	b/b'	c/c'	1	2	3/4	5	6
20	31	29/31	22	22	25/23	25	23
100	30	31	25	56	65	73	97

Considering first the line positions observed using the various pulse sequences employed it may be seen that there are a number of spectral changes upon increasing the temperature above 80°C. It is significant that the first changes are apparent at temperatures which are *c.* 10°C below the calorimetric onset of the crystal–mesophase transition, thus suggesting some pre-transitional effects. The most obvious changes

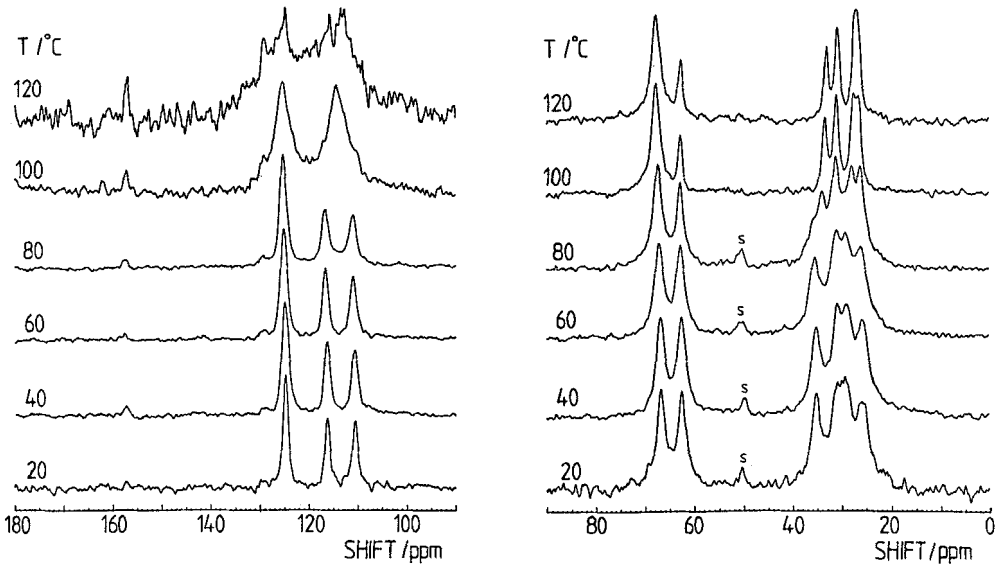

Figure 9. Variable temperature SC ^{13}C spectra for BHHBP. The peaks denoted s are due solely to spinning sidebands.

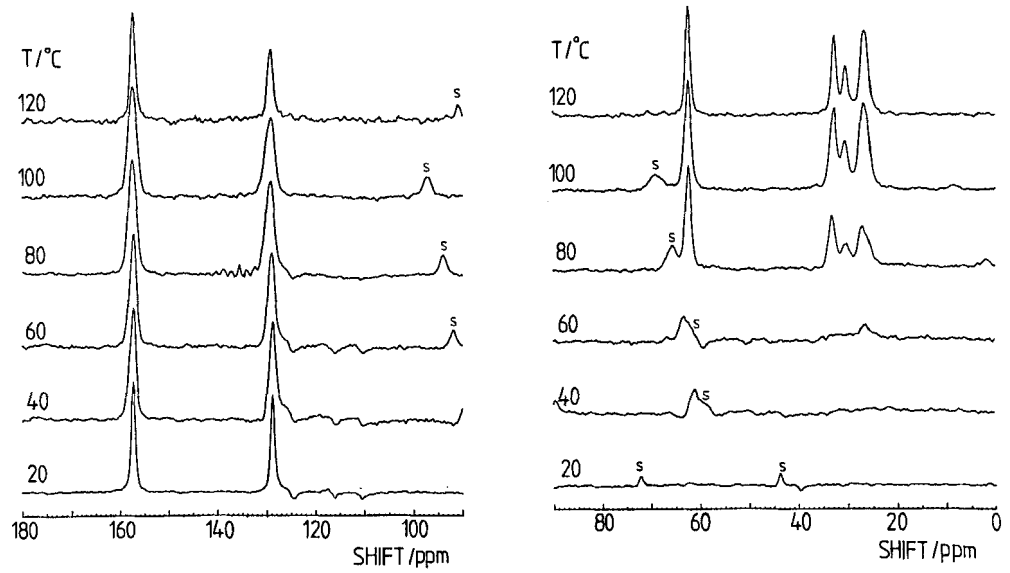

Figure 10. Variable temperature DD ^{13}C spectra for BHHBP. The peaks denoted s are due solely to spinning sidebands.

are in the aromatic region of the spectrum where the splitting of the aromic pair c/c' disappears above 80°C to produce a single line at a central position. Using a non-linear least squares technique, it was found that this new line could be fitted to a single lorentizian line quite satisfactorily, whereas no adequate fit could be obtained by superimposing a pair of lorentizian or gaussian lines with the former solid state splitting of *c.* 6 ppm. Both this line and the line arising from the other protonated

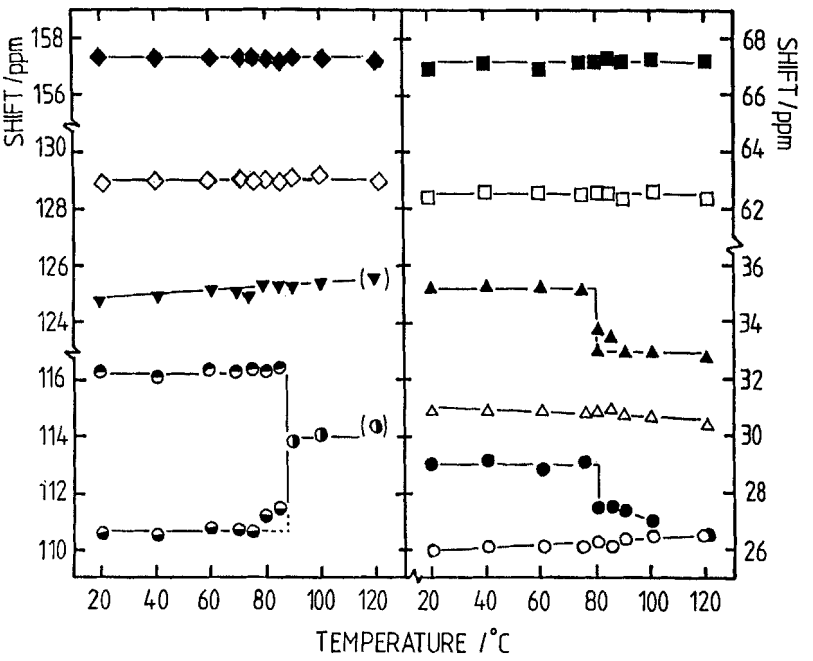

Figure 11. Collated ^{13}C chemical shift versus temperature data for BHHBP.

carbon pair *b*/*b*′ exhibit severe broadening at temperatures above 80°C while both of the non-protonated lines remain relatively sharp. The sources of line broadening in solid state CP/MASS spectra have been reviewed by VanderHart *et al.* [50]. Severe broadening can arise from modulation of the chemical shift anisotropy by molecular motion at frequencies close to the sample spinning frequency and from modulation of the ^{13}C–^{1}H dipolar coupling at frequencies close to the decoupler field strength expressed in frequency units. The latter effect has also been discussed by Lauprêtre *et al.* [51] in relation to the broadening of protonated side group carbons in poly(cyclohexyl methacrylate). In view of the fact that only the protonated carbons are broadened in the present instance it would appear that broadening by modulation of the ^{13}C–^{1}H interaction is dominant in the present instance. In such a case, for an aromatic C–H bond length of 1·02 Å, it is necessary to postulate a minimum ring librational motion of *c.* 20° rms in order to account for the 7·9 ppm excess broadening observed at 120°C for the protonated biphenyl carbons corresponding to a contribution of 0·8 ms to ^{13}C transverse relaxation time. Of course any larger scale motion which leads to an increased motional broadening effect such as free rotation or ring flips is also possible.

It may be noted that at 80°C the lines due to the aromatic carbon pair *c*/*c*′ are still relatively well resolved in the SC spectrum by comparison with the CP spectra at the same nominal temperature. This difference arises from the fact that the spectra were acquired on separate occasions and slight differences in the set point temperature probably occurred. An increase in temperature from 80°C to 82·5°C was sufficient to produce an SC spectrum with similar *c*/*c*′ lineshapes to those observed at 80°C in the CP spectrum.

More subtle changes can also be seen in the aliphatic region of the spectrum. As the temperature is increased the aliphatic line positions remain relatively unaffected

by temperature change until 80°C at which temperature the lines at 28·9 ppm and 35·3 ppm, assigned to carbons 3/4 and 5 respectively, shift to higher fields with increasing temperature until, eventually, the lines of the 3/4 carbon pair merge. The line at 67·7 ppm associated with carbon 1 also exhibits some broadening above 80°C, which is reminiscent of the broadening observed for the protonated aromatic carbons.

The observed shifts for the carbon lines at 35·3 ppm and 28·9 ppm in the solid state to higher fields in the mesophase must reflect specific steric effects which result from the change in the time averaged configurations of the molecules in the mesophase. Often the introduction of gauche defects into trans chain sequences are invoked to explain the mutual shielding of carbon pairs. In the present case, however, the two carbons involved, 3/4 and 5, are not thrice removed from each other and therefore cannot be involved in a mutual de-shielding γ-gauche type interaction. One might therefore speculate that these shift effects are intermolecular in origin. As was the case for the anomalous shift of the 25·7 ppm solid state line the interpretation of these effects must rely on a more detailed structural characterization of this material. Though it must be noted that even when detailed structural information is available the interpretation of intermolecular effects on ^{13}C carbon shifts can be difficult [52].

By comparison with the standard CP pulse sequence, the short contact time experiment preferentially polarizes those carbons which have strong carbon–proton couplings—namely the least mobile of the protonated carbons. In the dipolar dephasing experiment, on the other hand, the signal from those carbons with strong carbon–proton couplings is severely attenuated by the dipolar dephasing delay, thus selecting the carbons with weak carbon–proton dipolar couplings—the quaternery carbons and the protonated carbons which are most mobile. The relative intensities observed in the SC/CP and DD/CP spectra thus contain information pertaining to the relative mobility of the various protonated carbons in BHHBP. Below the crystal–mesophase transition the dipolar dephasing experiment indicates that all of the protonated carbons are immobile. Above 80°C, however, it is evident that motional averaging of the carbon–proton dipolar coupling is occurring. Table 6 presents the intensities of the various protonated carbons obtained at 100°C using the SC and DD pulse sequences relative to those obtained using the standard CP sequence after normalizing the intensity of the 62 ppm line to unity. For the SC/CP data in table 6 those carbons which are *least* mobile will have the largest relative intensities while for the DD/CP data the *most* mobile species will have the largest relative intensities. It is readily apparent that the SC and DD data lead to the same ranking of mobility for all of the protonated carbons and that this ranking is, in turn, consistent with the cross polarization data summarized in table 5 for which the most mobile carbons are expected to show the greatest increase in $t_{1/2}$ at 100°C compared to 20°C. On the basis of these results the various carbon species are ranked as follows in terms of

Table 6. Relative intensities for various carbon lines at 100°C.

	Relative intensity						
Experiment†	*b*/*b*′	*c*/*c*′	1	2	3/4	5	6
DD/CP	0	0	0	0·51	0·61	0·77	1·0
SC/CP	5·9	5·7	4·1	2·0	1·4	1·4	1·0

† CP = cross polarization, DD = dipolar dephasing, SC = short contact time experiment (see text).

mobility

$$6 > 5 > 4 \approx 3 > 2 \gg 1 \geqslant b/b', c/c'.$$

Thus it can be seen that, starting from the biphenyl core, mobility increases in a regular fashion on passing from the alkoxy carbon 1 to the hydroxy carbon 6.

The comparative rigidity of the alkoxy carbon 1 compared to the other aliphatic carbons is at once obvious from the data presented above. Indeed it would appear that the mobility of the biphenyl group is comparable to that of the alkoxy methylenes, suggesting that the locking effect noted in the solid state may still be largely effective in the mesophase.

The motional modes of the biphenyl mesogen, which from the above discussion appear quite restricted, are of particular interest and can be elucidated to some extent by the following observations:

(i) Broadening of the protonated carbon lines in the BHHBP mesophase results from fast ($\tau_c \approx 3\,\mu s$) motional modulation of the ^{13}C–^{1}H interaction [49].
(ii) The reduction in the strength of this dipole–dipole interaction due to motional averaging in the mesophase is small since the protonated aromatic carbon lines are eliminated from the DD spectra by the short 50 μs dephasing delay and have similar cross polarization times at 20°C and 100°C (table 5).
(iii) The collapse of the c/c' doublet at *c.* 80°C indicates that from an NMR perspective these carbons are equivalent.

Calculations of the effect of motional modulation upon the breadth of the protonated aromatic lines indicate that the observed broadening can be accounted for in terms of small 20° rms librations, continuous rotation, or ring flips of the biphenyl. However, both continuous rotation and ring flips lead to large reductions in the second moment of the ^{13}C–^{1}H dipole–dipole interaction by factors of 64 and 2·3, respectively. These values would be inconsistent with the near rigid lattice cross polarization times (table 5) which these carbons still exhibit at 100°C. This leaves the possibility of small librations of *c.* 20° rms which lead to a reduction in the second moment of the ^{13}C–^{1}H interaction by a factor of 1·2. Such small librations cannot, of course, serve to average the 6 ppm chemical shift difference between carbons c and c'. Since the averaging of a chemical shift difference of this magnitude can be achieved by much slower motional processes than those required to reduce the strength of dipole–dipole interaction, it is only necessary to postulate that, in addition to the fact librations of the biphenyl unit about its equilibrium orientation, 180° jumps occur at a slower rate ($\tau_c \leqslant 3$ ms) effecting interchange of the c/c' sites.

Of course other schemes could be imagined for accounting for the observed collapse of the c/c' pair. A reorientation of the biphenyl to a new equilibrium position such that the alkoxy group is equally disposed toward each carbon of the c/c' pair and small torsional oscillations of the biphenyl about this new position could be expected to produce similar effects. Such a structural change should lead to a reduction in the steric interaction between hydrogen atoms bonded to the alkoxy carbon and the ortho ring carbon of the biphenyl and thus produce a de-shielding of the alkoxy carbon resonance—which is not observed. Uryu and Kato [39, 40], for example, have reported a downfield shift of *c.* 1·5 ppm accompanying a change from an in-plane to an out-of-plane conformation for an alkoxy group relative to an aromatic ring in thermotropic polyester compounds. The ring flip mechanism is also favoured by the observation, made earlier in the discussion, that the relative rigidity of the alkoxy

carbon compared to the other carbons suggests that the locking effect of the alkoxy carbon relative to the biphenyl is still effective in the mesophase.

Considering all of the experiments outlined above it is clear that BHHBP exhibits a stable mesophase above 97°C and that this mesophase is highly ordered. Although a complete structure analysis is not available for either crystal or mesophase considerable insight can nevertheless be gained into the arrangement of molecules in these phases. For the crystalline phase infrared data indicate that the alkyl chains have an all-trans conformation. Additionally NMR spectra show that the alkyl chain is co-planar with the plane of the aromatic ring suggesting an overall all-trans conformation of the molecule. X-ray data also indicate that the long axis of the BHHBP molecules are inclined at an angle of 45°–55° to the crystal layer plane.

Upon passing into the mesophase some pre-transitional effects are apparent in the infrared and NMR spectra recorded at 80°C suggesting that the DSC transition which has its onset at *c.* 90°C has its origin in internal motions of the BHHBP molecule which set in at lower temperature. Once in the mesophase, infrared and X-ray data indicate that the all-trans configuration of the alkyl chain is still preferred and that the molecule still maintains an appreciable tilt to the plane normal. Despite these observations there is considerable evidence from NMR to indicate appreciable motional effects in the BHHBP mesophase. The biphenyl moiety remains relatively constrained in the mesophase, at least up until 120°C, and exhibits only small angle torsional motions at an appreciable rate, with perhaps ring flips occurring at a much slower rate. This same lack of mobility also attaches to the alkoxy carbon of the alkyl spacer suggesting that there is still some locking effect between the alkoxy group and the biphenyl in the mesophase. The other methylene units in the alkyl spacer are, by comparison with the biphenyl core and the alkoxy carbons, much more mobile and exhibit appreciable dispersion in terms of mobility. The mobility, as probed by the motional averaging of the ^{13}C–^{1}H dipole–dipole interaction, is seen to increase in a systematic fashion from the biphenyl core to the hydroxy end of the molecule.

In view of the fact that the biphenyl cores do not behave as free rotors, but rather exhibit only restricted re-orientational motions it would appear that none of the smectic phases which exhibit hexagonal or pseudo-hexagonal symmetry can be compared with the mesophase of BHHBP. Rather, it appears reasonable to associate BHHBP with that class of mesophase to which Leadbetter [4], in his review of liquid crystal phases, assigns the term 'disordered crystals', namely the tilted smectic J and K phases which exhibit a herringbone type of packing and symmetry with respect to 180° rotation about the molecular axis.

4. Conclusions

BHHBP exhibits a stable highly ordered S_G or S_H mesophase between 97°C and 179°C. In both the low temperature crystal phase and the higher temperature mesophase the molecules are inclined at an appreciable angle to the layer normal. The mesophase is distinguished from the crystal phase by the onset of considerable mobility in the alkyl chains following the alkoxy carbon and by fast small angle librations of the biphenyl moiety. The alkoxy carbons adjacent to the biphenyl core, are like the core itself, severely restricted in terms of mobility by comparison with the rest of the molecule. In general, motional freedom is found to be most restricted at the biphenyl core and to increase in a systematic fashion towards the periphery of the molecule.

The authors wish to thank Mr. Peter Stenhouse and Mr. Fotios Papadimetrikapolous for supplying samples of BHHBP used in this study. One of us (G.S.) wishes to thank Drs. J. C. W. Chien and L. C. Dickenson for access to their NMR facilities and for useful discussion, and Dr. D. Rice who provided the BHHBP solution NMR spectra. We also wish to acknowledge funding provided by CUIMRP at the University of Massachusetts and the Army Research Office, Grant ARO 23941-CH.

References

[1] DEVRIES, A., 1979, *Liquid Crystals: the Fourth State of Matter*, edited by F. D. Saeva (Marcel Dekker).
[2] WUNDERLICH, B., MÖLLER, M., GREBOWICZ, J., and BAUER, H., 1988, *Advances in Polymer Science*, Vol. 87 (Springer-Verlag).
[3] SACKMANN, H. (editor), 1985, *Sixth Liquid Crystal Conference of Socialist Countries*, Halle.
[4] LEADBETTER, A. J., 1987, *Thermotropic Liquid Crystals*, edited by G. W. Gray (Society of Chemical Industry).
[5] GRAY, G. W., and GOODBY, J. W G., 1984, *Smectic Liquid Crystals—Textures and Structures* (Leonard Hill).
[6] CHANDRASEKHAR, S., 1988, *Contemp. Phys.*, **29**, 527.
[7] SAMULSKI, E. T., DYBOWSKI, C. R., and WADE, G. E., 1972, *Phys. Rev. Lett.*, **29**, 340; 1972, *Ibid.*, **29**, 1050.
[8] WROBEL, S., JANIK, J. A., MOSCICKI, J., and URBAN, S., 1975, *Acta phys. pol.* A, **48**, 215.
[9] JANIK, J. A., and JANIK, J. A., 1985, *Sixth Liquid Crystal Conference of Socialist Countries*, edited by H. Sackmann, Halle.
[10] CZAPLICKI, J., and PISLEWSKI, N., 1985, *J. magn. Reson.*, **63**, 31.
[11] DONG, Y. D., 1986, *J. magn. Reson.*, **66**, 422.
[12] POLLACK, S. K., SHEN, D. Y., WANG, Q., STIDHAM, H. D., and HSU, S. L., 1989, *Macromolecules*, **22**, 551.
[13] STENHOUSE, P. J., VALLÉS, E. M., MACKNIGHT, W. J., and KANTOR, S. W., 1989, *Macromolecules*, **22**, 1467.
[14] SHEN, D. Y., POLLACK, S. K., and HSU, S. L., 1989, *Macromolecules*, **22**, 2564.
[15] SMYTH, G., VALLÉS, E. M., POLLACK, S. K., GREBOWICZ, J., STENHOUSE, P. J., HSU, S. L., and MACKNIGHT, W. J., *Macromolecules* (to be published).
[16] RECK, B. and RINGSDORF, H., 1985, *Makromolek. Chem. rap. Commun.*, **6**, 291; 1985 *Ibid.*, **6**, 691.
[17] RECK, B., and RINGSDORF, H., 1987, *Makromolek. Chem. rap. Commun.*, **7**, 389.
[18] SATO, M., NAKATSUCHI, K., and OHKATSU, Y., 1986, *Macromolek. Chem. rap. Commun.*, **7**, 231.
[19] SHAEFER, J., STEJSKAL, E. O. and BUCHDALL, R., 1977, *Macromolecules*, **10**, 384.
[20] HAVENS, J. R., and KOENIG, J. L., 1983, *Applied Spectroscopy*, **37**, 226.
[21] OPELLA, S. J. and FREY, M. H., 1979, *J. Am. chem. Soc.*, **101**, 5854.
[22] MAYO, S. L., OLAFSON, BARRY D., and GODDARD, W. A., III, 1988, *Biograf*™ *Reference Manual*, Version 2.0, Appendix L.
[23] WUNDERLICH, B., 1980 *Macromolecular Physics*, Vol. 3 (Academic Press).
[24] GALBIATI, E., and ZERBI, G., 1986, *J. chem. Phys.*, **84**, 3509.
[25] GALBIATI, E., and ZERBI, G., 1986, *J. chem. Phys.*, **87**, 3653.
[26] BULKIN, B. J., 1976, *Advances in Liquid Crystals*, **2**, 199.
[27] KARDAN, M., REINHOLD, B. B., HSU, S. L., THAKUR, R., and LILLYA, C. P., 1986, *Macromolecules*, **19**, 616.
[28] SYNDER, R. G., and SCHACHTSCHNEIDER, J. H., 1963, *Spectrochem. Acta*, **19**, 85.
[29] PIMENTAL, G. C., and MCCLELLAN, A. L., 1960, *The Hydrogen Bond* (Reinhold).
[30] SILVERSTEIN, R. M., BASSLER, G. C., and MORRILL, TERENCE C., 1974, *Spectroscopic Indentification of Organic Compounds*, third edition (John Wiley & Sons), p. 101.
[31] EATON, V. J., and STEELE, D., 1973, *J. chem. Soc. Faraday Trans. II*, **69**, 1601.
[32] BARRETT, R. M., and STEELE, D., 1972, *J. molec. Struct.*, **11**, 105.
[33] KUCHARSKI, S. A., and CZUCHAJOWSKI, L., 1979, *J. molec. Struct.*, **55**, 103. (a) SCHMID, E. D., and BROSA, B., 1972, *J. chem. Phys.*, **56**, 6267.

[34] PAINTER, P. C., COLEMAN, M. M., and KOENIG, J. L., 1982, *The Theory of Vibrational Spectroscopy and its Application to Polymeric Materials* (Wiley–Interscience).
[35] KEMP, W., 1986, *NMR in Chemistry: A Multinuclear Introduction* (Macmillan).
[36] 1978, *Sadtler Standard Carbon-13 NMR Indexes* (Sadtler Research Laboratories Inc.).
[37] LIPPMAA, E. T., ALLA, M. A., PEHK, J. J., and ENGELHARDT, G., 1978, *J. Am. chem. Soc.*, **100**, 1929.
[38] MARICQ, M. M., and WAUGH, J. S., 1979, *J. chem. Phys.*, **70**, 3300.
[39] URYU, T., and KATO, T., 1987, *Chem. Lett.*, p. 211.
[40] URYU, T., and KATO, T., 1986, *Macromolecules*, **21**, 378.
[41] KATO, T., KABIR, G. M. A., and URYU, T., 1989, *J. Polym. Sci. Chem. Ed.*, **27**, 1447.
[42] TONELLI, A. E., and SCHILLING, F. G., 1981, *Accts Chem. Res.*, **14**, 233.
[43] AXELSON, D. E., 1986, *High Resolution NMR Spectroscopy of Synthetic Polymers in Bulk*, edited by R. A. Komoroski (VCH Publishers).
[44] MULLER, L., KUMAR, A., BAUMANN, T. and ERNST, R. R., 1974, *Phys. Rev. Lett.*, **32**, 1402.
[45] CHEUNG, T. T. P., and YARIS, R., 1980, *J. chem. Phys.*, **72**, 3604.
[46] ABRAGAM, A., 1961, *The Principles of Nuclear Magnetism* (Oxford University Press).
[47] LAUPRÊTRE, F., NOËL, C., JENKINS, W. N., and WILLIAMS, G., 1985, *Faraday Discuss. chem. Soc.*, **79**, 191.
[48] LAUPRÊTRE, F., MONNERIE, L., and VIRLET, J., *Macromolecules*, **17**, 1397.
[49] VAN VLECK, J. H., 1948, *Phys. Rev.*, **74**, 1168.
[50] VANDERHART, D. L., EARL, W. L., and GARROWAY, A. N., 1981, *J. magn. Reson.*, **44**, 361.
[51] LAUPRÊTRE, F., VIRLET, J., and BAYLE, J. P., 1985, *Macromolecules*, **18**, 1846.
[52] VANDERHART, D. L., 1981, *J. magn. Reson.*, **44**, 117.